catalysts

MDPI

Article

Selective Oligomerization of Isobutylene in Mixed C4 with Co/BETA-Loaded Molecular Sieve Catalysts

Xiaoping Chen [1,2], Panhu Yu [2], Hui Tian [2] and Shuguang Xiang [1,*]

[1] College of Chemical Engineering, Qingdao University of Science and Technology, Qingdao 266042, China
[2] College of Chemistry and Chemical Engineering, Yantai University, Yantai 264005, China
* Correspondence: xsg@qust.edu.cn

Abstract: This paper investigates the use of loaded Co/BETA molecular sieve catalysts for the selective oligomerization of isobutylene. The physicochemical properties of Co/BETA molecular sieves were characterized using XRD, BET, NH3-TPD, FT-IR, XPS, and Py-FTIR. The effects of different active component loadings, reaction temperatures, and reaction air velocities on the selective oligomerization of isobutylene were investigated in a fixed-bed reactor. The results showed that the catalytic effect was optimal when the Co loading was 6%, the reaction temperature was 60 °C, the reaction pressure was 1 MPa, and the reaction air speed was 1 h^{-1}. The isobutylene conversion was greater than 74%, the $C_8^=$ selectivity was approximately 70%, and the $C_8^=$ yield reached 51.69% with minimal loss of n-butene, providing good catalytic capacity and efficiency.

Keywords: isobutylene; oligomerization; selectivity; n-butene

check for updates

Citation: Chen, X.; Yu, P.; Tian, H.; Xiang, S. Selective Oligomerization of Isobutylene in Mixed C4 with Co/BETA-Loaded Molecular Sieve Catalysts. *Catalysts* **2024**, *14*, 533. https://doi.org/10.3390/catal14080533

Academic Editor: Narendra Kumar

Received: 10 July 2024
Revised: 26 July 2024
Accepted: 12 August 2024
Published: 16 August 2024

1. Introduction

Mixed C4 is a significant chemical resource that is produced as a by-product of catalytic cracking and steam cracking processes. The substance comprises a significant quantity of readily accessible C4 olefins [1–3]. The catalytic cracking process serves as the foundation of China's petrochemical sector, resulting in a significant production of C4 olefins as a by-product. The majority of the isobutylene found in C4 olefins is utilized for the production of methyl tert-butyl ether (MTBE) [4]. The need for enhanced petrol components has arisen due to the combination of environmental restrictions and the automotive industry's growing demand for unleaded petrol for automobiles [5]. Because of its high water solubility and low volatility, MTBE is difficult to decompose and rapidly pollutes the environment [6,7]. Due to societal progress and the increasing demand for a healthier environment, the utilization of MTBE will unavoidably diminish or may be prohibited. This occurrence results in a significant excess of isobutylene [8]. The process of selectively combining isobutylene molecules to form oligomers is used to efficiently separate n-butene from a mixture of C4 compounds. Furthermore, it has the capability to substitute the MTBE process. The C8 olefin resulting from the oligomerization of isobutylene is further subjected to hydrogenation to obtain iso-octane [9], which is a petrol additive possessing a high octane rating. Substituting MTBE with iso-octane is a highly efficient method to enhance the composition of petrol. Therefore, the selective oligomerization of isobutylene provides a significant opportunity for the usage of mixed C4.

Isobutylene oligomerization is a process that is catalyzed by an acid. Brönsted acid or Lewis acid on the catalyst can induce isobutylene oligomerization. The research on olefin oligomerization technology in foreign countries started pretty early, and the processing equipment is also relatively advanced. Some of the traditional olefin process technologies include the non-selective stacking process (SPAC) developed by Global Petroleum Corporation (UOP) in the United States, the MOGD process developed by Mobil Petroleum Corporation (Mobil), and the Difasol olefin oligomerization process developed by the French

Institute of Petroleum (IFP). The catalyst plays a crucial role in this reaction. Previously, liquid acid catalysts were used to catalyze oligomerization reactions [10,11]. Nevertheless, the system's inadequate segregation and inclination to cause equipment corrosion have restricted its progress in the industry. Currently, the predominant catalysts employed in industry are solid acid catalysts, such as solid phosphoric acid [12], acid resins [13–15], and molecular sieve catalysts [16–18], which have extensive applications. Mohammed and his colleagues (Mohammed et al. [19]) synthesized novel eco-friendly catalysts by impregnating HY zeolites with phosphoric acid. Studies have demonstrated that this catalyst consistently achieves a conversion rate of isobutylene ranging from 97 to 100%, while exhibiting a maximum selectivity of 65% for C8. The catalyst has a lifespan exceeding 21 months. The authors of the study are Huo Wentao et al. [20]. This study performed comprehensive comparative analyses on various molecular sieves exhibiting distinct topological structures, namely EUO, MOR, Beta, and MWW. Studies have discovered that when isobutene undergoes the oligomerization reaction, the MWW molecular sieve achieves an 80% conversion rate of isobutene and 55% selectivity for carbon eight olefins. These results were obtained under reaction conditions of a 0.5 MPa pressure, a 160 °C temperature, and a mass space velocity of 20 h^{-1}. Yu Yue et al. [21] investigated the impact of Ni alteration on the isobutene oligomerization reaction using the HZSM-5 catalyst. Studies have demonstrated that with a loading level of 0.25% of Ni, the carbon octaolefin yield reaches 45%. The characterization results demonstrate that the addition of Ni can enhance the Lewis/Brønsted ratio, and the presence of Ni species and Al in HZSM-5 may lead to the formation of $NiAl_2O_4$.

In recent years, ionic liquid catalysts [22,23] have emerged and been used in olefin oligomerization reactions. However, ionic liquids suffer from high mass transfer resistance and poor stability in catalytic butene oligomerization reactions. Chen et al. [24] investigated whether the addition of emulsifiers to ionic liquids can form eutectic microemulsions that can enhance the effective contact between butene and the catalyst. Butylene can be converted up to 98% and dimer selectivity up to 91%. Júlia et al. [25] have studied ionic liquids with different types of emulsifiers and loaded onto silica. It was found that these catalysts can perform oligomerization reactions under milder conditions. Furthermore, the Brønsted acidic imidazole ionic liquids can be replaced by SILPs containing less toxic non-aromatic cations. In addition, these catalysts were found to be extremely sensitive to water. Some researchers have reported the application of heteropolyacids [26,27] or acidic metal–organic frameworks [28,29] to olefin oligomerization reactions.

Joanna et al. [30] studied a series of oxovanadium complexes and used them to catalyze the polymerization reaction of olefin monomers. The oxovanadium complexes have very high catalytic properties in both 2-chloro-2-propen-1-ol polymerization and 3-buten-2-ol polymerization. The most active catalyst measured by the addition of an activator was [VO-(dipic)(bipy)]/$EtAlCl_2$, which was active up to 11,040 kg/(molV^{-h}) at 60 °C and had good thermal stability. Yu et al. [31] realized an isobutylene-selective zwitterionic polymerization reaction on modified β molecular sieves by adding ethanol to the feedstock. They combined reactive distillation techniques to simulate and optimize the process. This use of reactive distillation to simulate isobutylene zwitterionic reactions also provides ideas for simulating other olefinic zwitterionic reactions.

Yu et al. [32] studied and characterized loaded metal sulfate catalysts. It was shown that the $Fe_{0.2}Zn_{1.8}/SiO_2$ catalyst was able to achieve an isobutylene conversion rate of 89%, an n-butylene conversion rate of 0%, and C8 selectivity of 57%. And after 50 h of continuous operation, the isobutylene conversion rate can be maintained at more than 80%. The authors concluded that metal loading on molecular sieve catalysts is important for the selective oligomerization reaction of isobutylene. The BETA molecular sieve has a unique and unobstructed pore system, as well as adjustable acidity and good hydrothermal stability. It also has the advantages of high catalytic activity, strong anti-toxicity, and high stability. The addition of Co onto BETA molecular sieves can efficiently inhibit the elongation of polymer chains and enhance the selectivity toward C8 compounds by utilizing the redox capabilities

of Co^{3+} and Co^{2+}. The presence of cobalt oxide on the catalyst surface can modulate the surface acidity of the catalyst, hence diminishing the reactivity of n-butene and effectively suppressing the n-butene reaction.

Several studies have indicated that cobalt nitrate undergoes complete decomposition at around 200 °C, resulting in the formation of Co_3O_4 and CoO particles [33]. When subjected to a pre-treatment process in helium at a temperature of 550 °C, a portion of the cobalt oxide undergoes reduction and is transformed into metallic cobalt. Scientists documented the impact of catalysts containing cobalt oxide that had been subjected to high-temperature treatment on the process of ethylene oligomerization. Studies have discovered that subjecting catalysts to elevated temperatures leads to the production of a greater amount of linear alpha olefins, hence increasing their oligomerization activity. The cobalt phase present on the catalyst surface corresponds to CoO. The catalyst, following acid washing treatment, enhances the oxygen content by oxidizing surface functional groups. This process results in the isomerization of alpha olefins into inner olefins and inhibits the activity of oligomerization [34]. There has been limited research on the application of cobalt loaded on molecular sieves for the specific oligomerization of isobutylene.

The selective oligomerization process of isobutene in mixed C4 mainly involves a series of complex polymerization reactions of isobutene catalyzed by the acidic center of the catalyst. Due to the various types of mixed C4 and the complex process of selective oligomerization of isobutene, we simplified the selective oligomerization reaction system of isobutene in mixed C4 and drew a simple reaction schematic diagram, as shown in Figure 1.

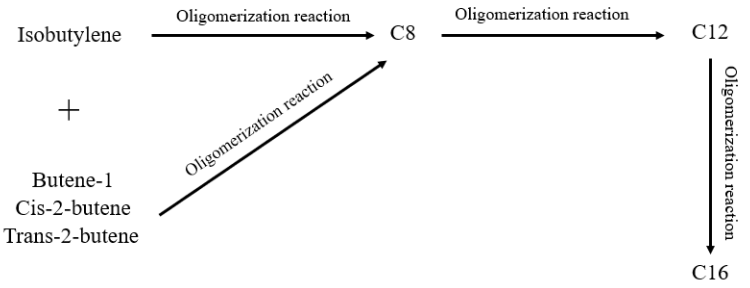

Figure 1. Schematic diagram of oligomerization reaction.

For this investigation, we prepared loaded Co/BETA molecular sieve catalysts through impregnation with Co $(NO_3)_2$ using a BETA molecular sieve as a carrier. The physicochemical properties of the loaded Co/BETA molecular sieves were characterized using XRD, BET, NH3-TPD, FT-IR, XPS, and Py-FTIR. The effects of the impregnation amount of Co, reaction temperature, and reaction air velocity on the conversion of isobutylene and n-butene and the reaction products were investigated using mixed C4 as the raw material.

2. Results and Discussion

2.1. Characterization of the Catalyst

2.1.1. XRD Analysis

Figure 2 shows a comparative XRD plot of the loaded Co/BETA molecular sieve catalysts with different loadings. Compared with the XRD diffraction pattern of the original BETA molecular sieve, the XRD diffraction pattern of the loaded cobalt metal shows characteristic diffraction peaks belonging to the BETA molecular sieve at 2 θ = 7.7° and 22.2°. However, it was observed that there was a significant decrease in the intensity of the two characteristic peaks of the BETA molecular sieve loaded with the active component, indicating that the loading of the active component affects the lattice strength of the BETA molecular sieve. The 8% Co sample showed two weak diffraction peaks of 36.8° and 65.2° [35], corresponding to the Co_3O_4 phase, demonstrating that loaded Co/BETA molecular sieves formed Co_3O_4 species when calcined in an air atmosphere. In addition, when the loading of Co was less than 6%, no characteristic diffraction peaks of the Co phase

were found, probably because the Co phase was uniformly dispersed on the surface of the BETA molecular sieve carrier [36].

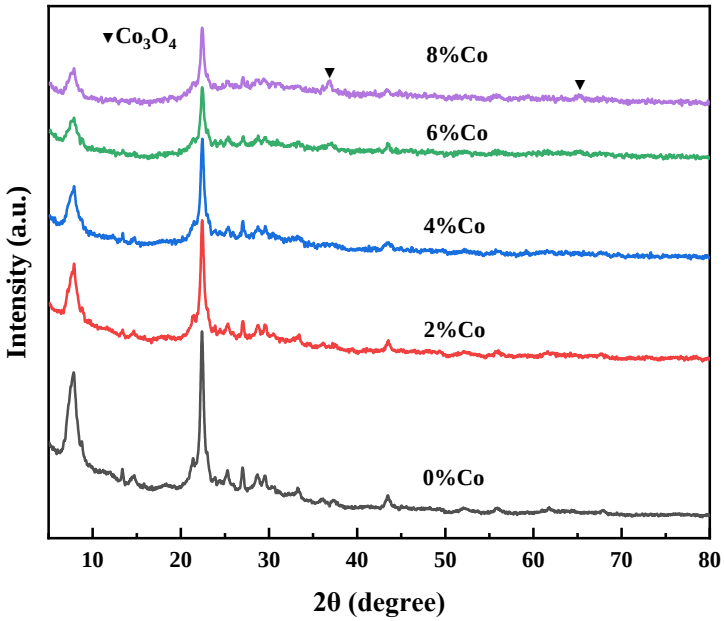

Figure 2. XRD spectra of catalysts with different active component loadings.

2.1.2. BET Analysis

The results of the specific surface area and pore structure of the catalysts with different Co loading amounts are shown in Figure 3 and Table 1. From Figure 3, it can be seen that the N_2 adsorption–desorption isotherms of the catalysts with different Co loading levels all exhibit type II adsorption, with a hysteresis loop of H1 type. This indicates that the mesoporous structure remains ordered after the introduction of Co onto the BETA molecular sieve. From Figure 3B and Table 1, it can be seen that the molecular sieve catalyst has microporous and mesoporous structures, with mesopores being the main component. With the increase in Co loading, the microporous structure gradually decreases, which may be due to the blockage of some micropores by the loaded Co oxide. The specific surface area and pore volume of the catalyst significantly decrease with the increase in Co loading, while the pore size gradually increases. The possible reason is that Co is incorporated into the BETA molecular sieve framework during the heating process of the muffle furnace, forming Co-O or Si-O-C_O bonds. In contrast, the bond length of Co-O is larger than that of Si-O [37], leading to an increase in pore size.

Table 1. Pore structure parameters of catalysts with different active component loadings.

Catalyst	Specific Surface Area (m^2 g^{-1})	Pore Size (nm)	Pore Volume (mL g^{-1})		
			V_{total}	V_{micro}	V_{meso}
0%Co	423	3.26	0.33	0.15	0.18
2%Co	422	3.36	0.35	0.16	0.19
4%Co	391	3.43	0.32	0.14	0.18
6%Co	353	3.46	0.29	0.13	0.16
8%Co	341	3.5	0.29	0.12	0.17

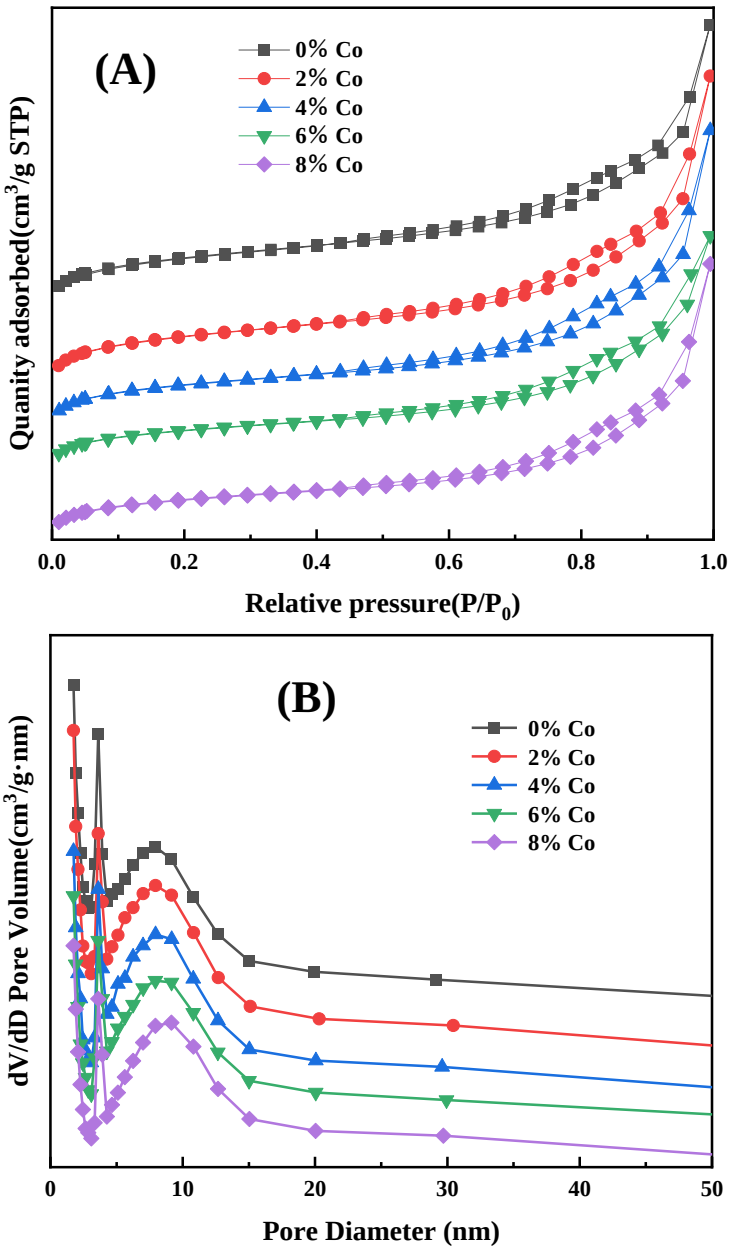

Figure 3. Adsorption–desorption isotherms (**A**) and pore size distribution maps (**B**) of catalysts with different Co loading levels.

2.1.3. NH_3-TPD Analysis

Figure 4 shows the NH_3-TPD results for the catalysts with different active components. The NH_3-TPD map may be related to the number and intensity of acidic sites. Below 300 °C, characteristic desorption peaks were observed for all catalysts with different loaded active components. Two major desorption peaks were observed on the 0% Co catalyst at approximately 129 °C and 404 °C. The low-temperature desorption peak corresponds to the weak acid center and the high-temperature desorption peak corresponds to the strong acid center. The catalysts with 0% Co prefer to produce large amounts of C12 products and polymers with higher carbon numbers. This is because of their high peak intensity. This is in agreement with our experimental results. After loading the active ingredient, the weak acid centers all seem to move to higher temperatures, while the strong acid centers disappear significantly and the peak intensities are significantly reduced. This is attributed to the fact that the loading of the active component creates new acidic sites that override the acidic sites of the original molecular sieves, making the catalyst less acidic.

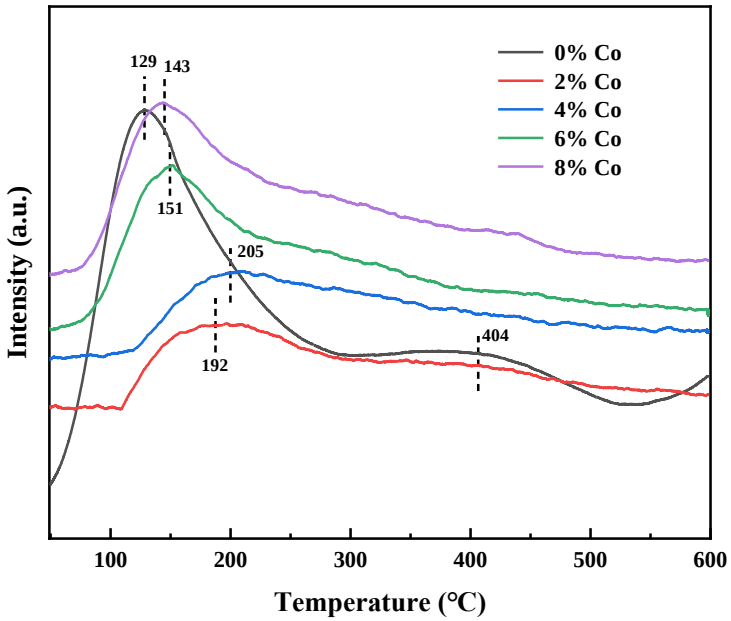

Figure 4. NH_3-TPD plots for catalysts with different active components.

2.1.4. FI-IR Analysis

Figure 5 displays the FT-IR spectra of BETA molecular sieves with varying amounts of cobalt loadings. The three absorption peaks observed at 573 cm^{-1}, 519 cm^{-1}, and 573 cm^{-1} can be attributed to the bending vibration of Si-O or Al-O. The absorption peaks at 1225 cm^{-1} and 1087 cm^{-1} are caused by the internally connected antisymmetric stretching motion of the TO4 (T = Si, Al) tetrahedron. The absorption peak at 796 cm^{-1} is due to the externally connected symmetric stretching vibration of TO4 [38]. The absorption maxima at about 3438 cm^{-1} and 1634 cm^{-1} are caused by the physical adsorption of water and the stretching vibrations of the O-H bonds in the surface silanol groups of the BETA molecular sieve [39]. The absorption peaks at around 1525 cm^{-1} and 1384 cm^{-1} are attributed to the presence of the -NO2 group. A possible cause is the utilization of cobalt nitrate as the impregnation solution, which, when subjected to the firing process in the muffle furnace, interacts with the catalyst and results in the absorption vibration peak of -NO2. The absorption peak at 667 cm^{-1} is attributed to the stretching vibration of Co-O or Si-O-Co [35]. This suggests that Co was integrated into the BETA molecular sieve structure during the calcination process, which aligns with the findings from the BET characterization.

2.1.5. Py-FTIR Analysis

In order to assess the acidity of the catalysts, we conducted pyridine infrared (IR) experiments on catalysts with 0% and 6% cobalt content. Figure 6 displays the results. The presence of pyridine uptake at the Brønsted and Lewis acidic sites can be identified by the absorption peaks at 1540 cm^{-1} and 1450 cm^{-1}, respectively. The absorption peak observed at 1480 cm^{-1} corresponds to the shared absorption peak of both Brønsted and Lewis acidic sites. Figure 6A demonstrates that the 0% Co catalyst possesses a higher quantity of Lewis acid sites and a lower quantity of Brønsted acid sites. Figure 6B demonstrates that the introduction of the Co active component leads to a notable reduction in Lewis acid and a substantial increase in Brønsted acid. Table 2 shows a drop in the overall acid content of the 6% Co catalyst, with a considerable decrease in Lewis acid and a significant increase in Brønsted acid. Additionally, the B/L value increases. The activity of isobutylene and n-butene is contingent upon the presence of a Lewis acidic site, as indicated by the evaluation results in Figure 7. Upon the introduction of the Co active component, the Co_3O_4 clusters exhibited a higher occupancy of Lewis acidic sites, resulting in a reduction in the quantity

of Lewis acid. Consequently, the activity of isobutylene decreased, leading to a drop in the conversion of isobutylene.

2.1.6. XPS Analysis

The elemental composition and chemical state of the 6% Co catalyst were analyzed by X-ray photoelectron spectroscopy. Figure 7A shows the elemental composition of the 6% Co surface corresponding to its binding energy labeling. The detailed Co 2p fitting results for the 6% Co catalyst are shown in Figure 7B. The sample can be fitted to six peaks attributed to Co^{3+}, Co^{2+}, and Co^{2+} satellite peaks, indicating the presence of Co^{2+} and Co^{3+} species on the catalyst surface [40]. The presence of satellite peaks at 787.1 eV indicates the presence of Co^{2+}, but the catalyst surface is dominated by Co^{3+}. The two peaks near 780.9 eV and 796.4 eV are attributed to the spin orbitals $Co2p_{3/2}$ and $Co2p_{1/2}$, respectively. The bimodal distance between $2p_{3/2}$ and $2p_{1/2}$ is 15.5 eV [39], which is consistent with the standard spectrum of elemental Co. No signal peak was found at 778 eV, proving the absence of Co monomers on the catalyst surface [41].

2.2. Catalyst Evaluation Results and Analysis

2.2.1. Evaluation Results of Different Co Loadings

The performance of catalysts containing various active components was assessed in a fixed-bed reactor, utilizing mixed C4 as the input material and a reaction temperature of 60 °C. The velocity of the air in the reaction was 1 h per hour, the pressure of the reaction was 1 megapascal, and the weight of the catalyst was 8 g. The assessment outcomes are depicted in Figure 8. The conversion exhibited a progressive decline as the active proportion increased. This phenomenon occurs due to the augmentation of the active component, which leads to the formation of more acidic sites on the catalyst's surface. The addition of new acidic sites will overlay the active sites on the original surface, resulting in a decrease in the specific surface area and pore volume of the catalyst. This also leads to an increase in pore size, which in turn reduces the contact area between isobutylene and the catalyst surface, ultimately impacting the efficiency of the catalytic process.

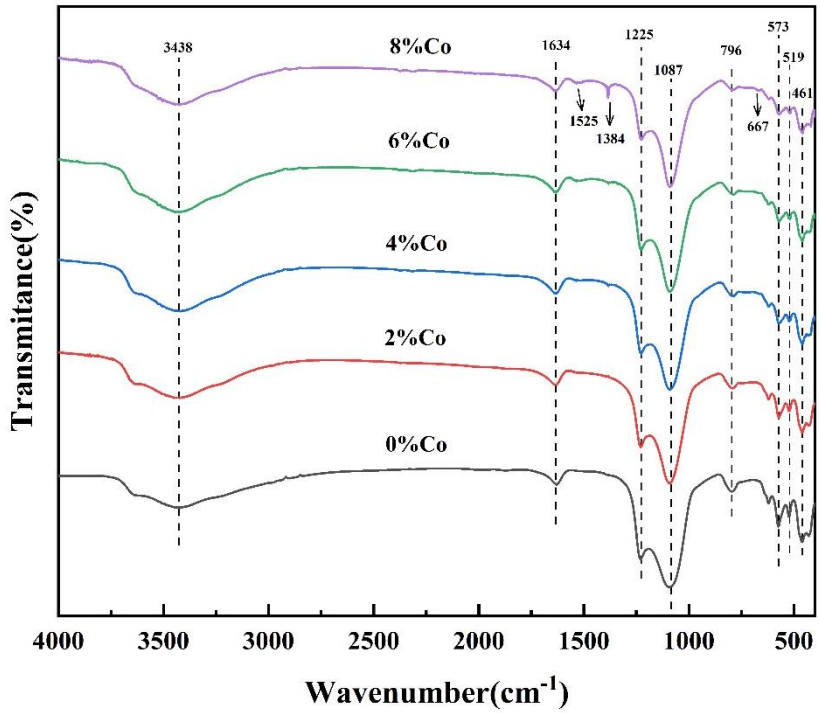

Figure 5. FT-IR plots of catalysts with different active components.

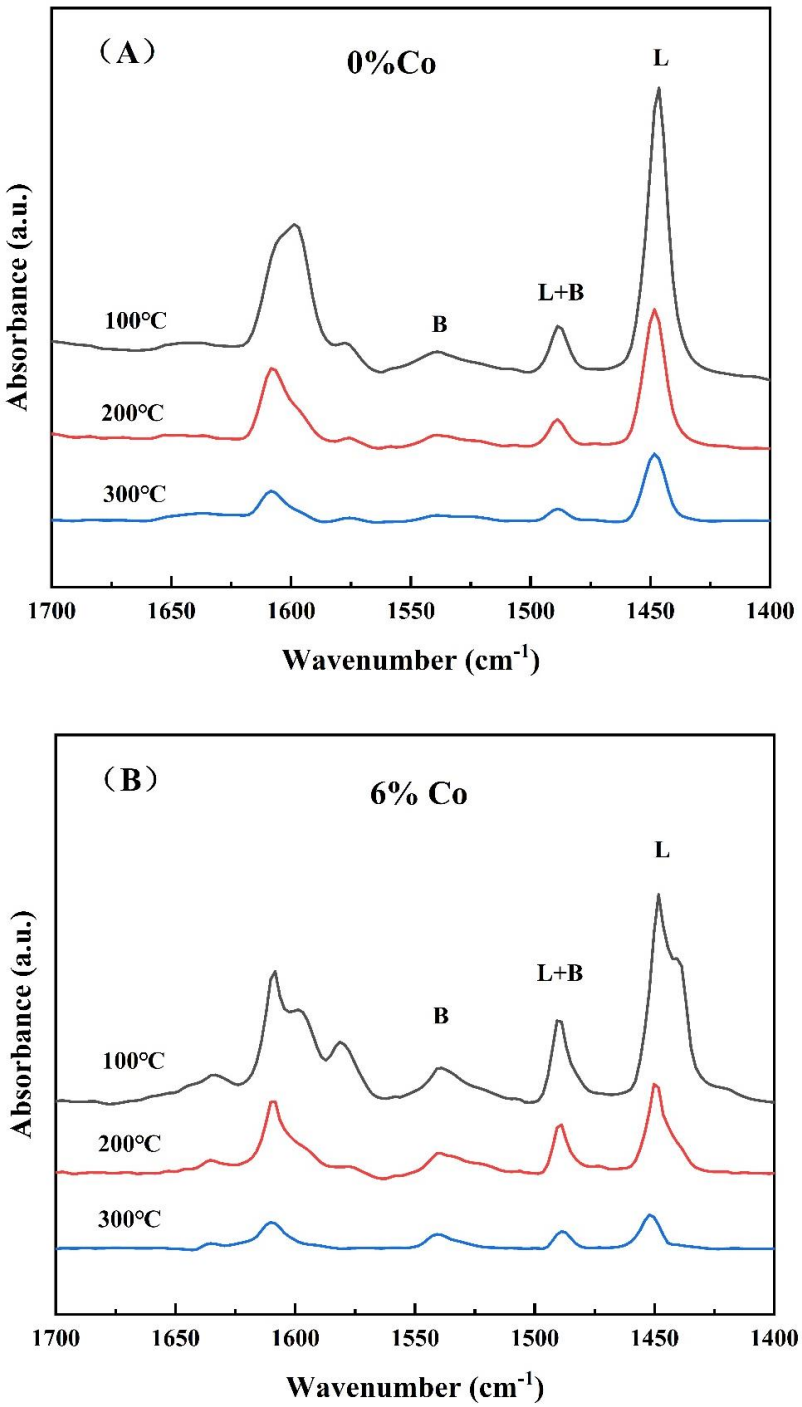

Figure 6. Py-FTIR spectra of (**A**) 0% Co and (**B**) 6% Co catalysts.

Table 2. Acid volume ratio of 0% Co and 6% Co catalysts.

Catalyst	0% Co				6% Co			
Temperature (°C)	Brønsted Acid	Lewis Acid	Total Acid Content	B/L	Brønsted Acid	Lewis Acid	Total Acid Content	B/L
100	21.48	129.17	150.65	0.17	30.76	116.50	147.26	0.26
200	12.56	58.77	71.33	0.21	24.07	37.16	61.23	0.65
300	7.70	29.17	36.87	0.26	10.37	12.89	23.26	0.81

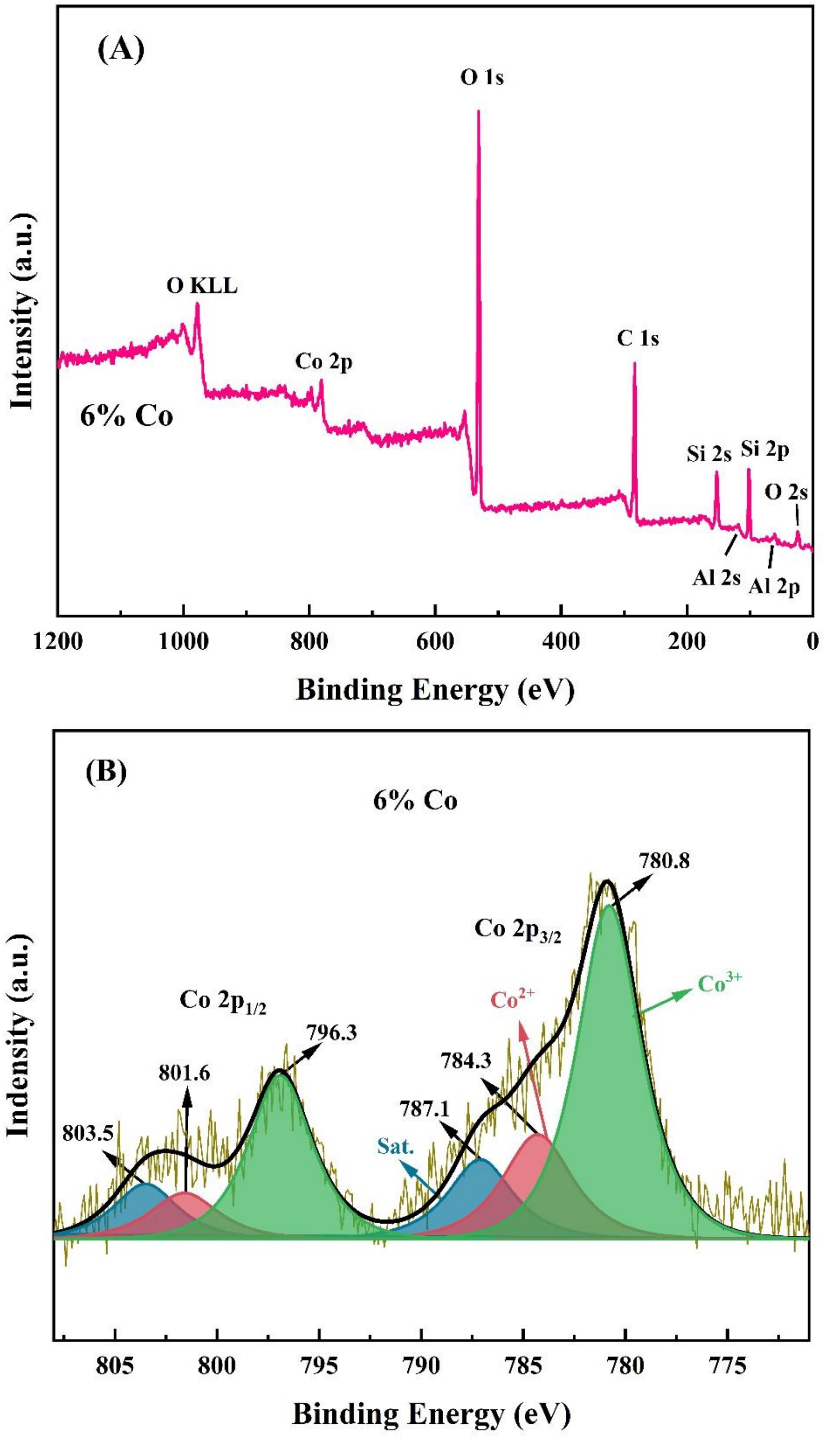

Figure 7. Scanning spectra of 6% Co catalyst (**A**) and Co 2p region (**B**).

This is consistent with the catalyst characterization results. The loaded active component is effective in inhibiting the growth of polymerization chains, leading to an increase in the selectivity of C8 polymers. The selectivity of C8 polymers reached 70% at 6% loading of active components. Secondly, the loss rate of n-butene is also important. It can be seen from the figure that the loss rate of n-butene showed a trend of decreasing and then increasing. The active sites on the surface of the BETA molecular sieve can be changed by the addition of active components, thus affecting the loss rate of n-butene. The lowest loss of n-butene was observed when the loading of Co was 6%. Increasing the loading of Co produces more active sites on the BETA molecular sieve and promotes the n-butene reaction.

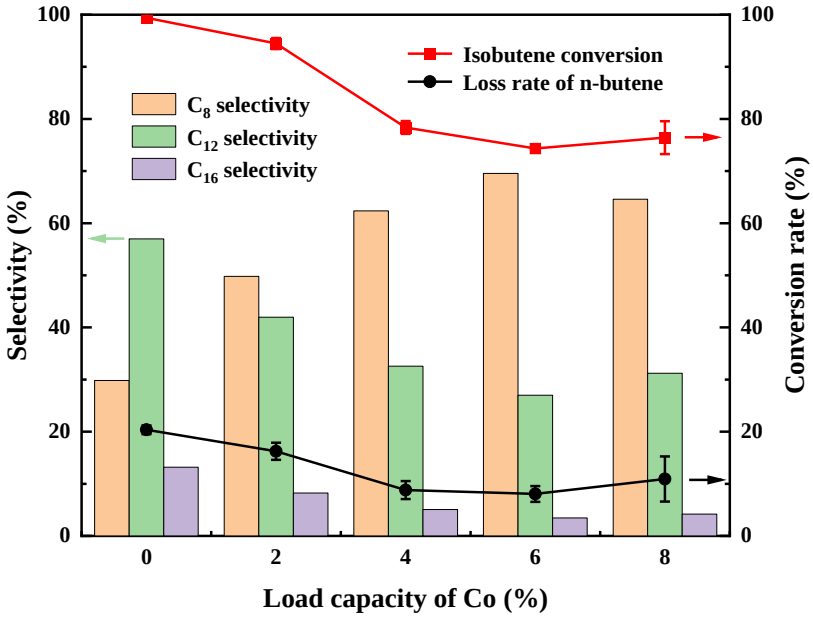

Figure 8. Evaluation results of loadings with different active components.

2.2.2. Evaluation Results of Different Reaction Temperatures

Catalysts which consisted of BETA molecular sieves with 6% Co loading were manufactured utilizing the same catalyst manufacturing processes. We ensured a consistent reaction pressure and reaction air velocity while modifying the reaction temperature. The results of the catalytic procedure are displayed in Table 3 and Figure 9. As the reaction temperature increased, the conversion of isobutylene showed a gradual increase, while the overall loss of n-butene remained consistently at around 10%. Table 3 demonstrates that the most significant C8 generation (51.69%) occurred when the reaction temperature was set at 60 °C, resulting in the lowest reduction in n-butene (8.11%). The loss rate of n-butene was significantly reduced compared to the catalytic results of the unloaded BETA molecular sieve. It is crucial to note that the dimer's selectivity decreases as the conversion of isobutylene steadily increases throughout the temperature range of 55–65 °C.

Table 3. Catalytic effect of 6% Co/BETA-loaded molecular sieve catalysts at different reaction temperatures.

Temperature/°C	Conversion/%		Selectivity/%			Yield of $C_8^=$/%
	Isobutylene	n-Butene	$C_8^=$	$C_{12}^=$	$C_{16}^=$	
50	57.87	8.23	66.58	28.50	4.92	38.53
55	60.40	10.71	73.55	23.19	3.26	44.42
60	74.34	8.11	69.54	27.01	3.45	51.69
65	80.48	12.53	57.01	35.65	7.34	45.88
70	80.19	9.50	59.87	30.35	9.78	48.01

The reason for this is that oligomerization events are irreversible exothermic reactions. The activation energy for the dimerization reaction of isobutylene and n-butene is 29 kJ/mol [15]. Additionally, the isobutylene oligomerization reaction is influenced by temperature, resulting in an enhanced conversion of isobutylene. Raising the reaction temperature enhances the reaction rate of oligomers, thereby reducing the proportion of dimers in the oligomers. The equilibrium conversion of isobutylene increases as the temperature rises due to the irreversible exothermic nature of the process. Conversely, the rise in temperature enhances the frequency of oligomerization reactions, leading to a propensity for greater formation of trimers or tetramers.

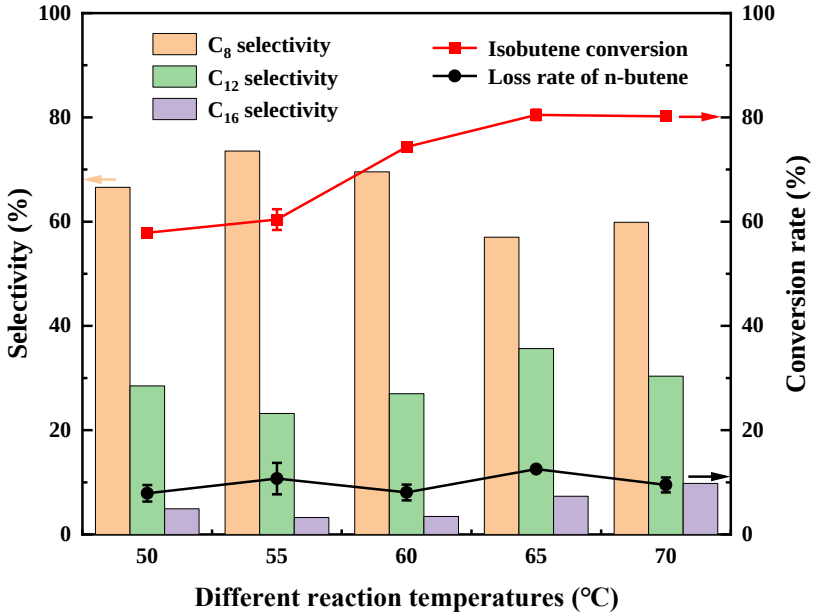

Figure 9. Catalytic results at different reaction temperatures for catalysts with 6% loading of active components.

2.2.3. Evaluation Results of Different Reaction Air Velocities

The reaction air velocity was varied while keeping the catalyst preparation method, reaction temperature, and pressure constant. The catalytic effect is shown in Figure 10. The conversion of isobutylene increases as the reaction air speed increases. The selectivity of C8 first increases and then decreases. The loss rate of n-butene increases at lower air speeds. At the equilibrium of the isobutylene reaction, an increase in residence time promotes the n-butene reaction, leading to an increase in the loss of n-butene. With the increase in air speed, the loss rate of n-butene decreases, and at an air speed of 1 h^{-1}, the loss rate of n-butene is the lowest, and the conversion rate of C8 selectivity and isobutylene reaches a good state. An increase in air velocity intensifies the polymerization reaction and leads to an increase in trimers.

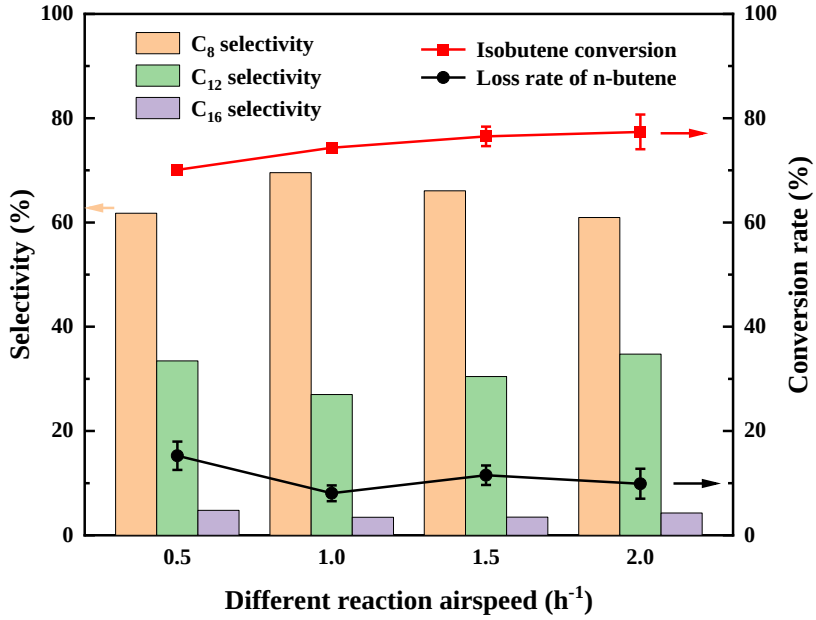

Figure 10. Evaluation results of catalysts with 6% active component loading at different reaction air velocities.

3. Materials and Methods

3.1. Experimental Materials

BETA molecular sieves (Si/Al = 25) were purchased from Nankai University Catalysts Ltd., Tianjin, China. Analytically pure Co $(NO_3)_2 \cdot 6H_2O$ was purchased from Sinopharm Chemical Reagent Co., Beijing, China Table 4 provides the composition of the experimental raw material blend C4.

Table 4. Composition of mixed C4 raw material.

Raw Material Composition	Propane	Propylene	Isobutane	n-Butane	trans-2-Butene	n-Butene	Isobutylene	cis-2-Butene
Mass fraction (%)	0.96	0.42	27.11	10.89	14.18	10.19	27.22	9.03

3.2. Catalyst Preparation

To eliminate impurities, the BETA molecular sieve was initially subjected to calcination in a muffle furnace at a temperature of 550 °C for a duration of 3 h. Subsequently, solids of Co $(NO_3)_2 \cdot 6H_2O$ with Co loading of m(Co)/m[m(Co $(NO_3)_2 \cdot 6H_2O$) + m(BETA)] = 0%, 2%, 4%, 6%, and 8% were dissolved in a suitable quantity of deionized water. The calcined BETA molecular sieves were soaked in a solution using the same volume as in the impregnation method and thoroughly mixed. The agitated mixture was thereafter secured onto the spinner and rotated at a temperature of 20 °C and a speed of 150 RPM for a duration of 2 h. The process involved spin-steaming the material at a temperature of 90 °C and a speed of 100 RPM for a duration of 1 h. The catalysts were dehydrated in a high-temperature oven at 120 °C for 3 h following spin-drying. Ultimately, the catalysts underwent the process of calcination in a muffle furnace at a temperature of 550 °C for a duration of 3 h, resulting in the production of Co/BETA-loaded molecular sieve catalyst samples.

3.3. Catalyst Characterization

3.3.1. XRD Analysis

The catalyst samples were characterized and tested using a SmartLab III X-ray diffractometer, Rigaku, Tokyo, Japan, to analyze the crystal phase and structure of the catalysts. Under the conditions of a scanning angle of 2θ = 5°–80°, a scanning speed of 10°/min, a working voltage of 45 kV, and a working current of 2000 mA, a Cu target (K α ray, λ = 1.5418 Å) was used as the radiation source.

3.3.2. BET Analysis

We conducted BET characterization testing using the Micromeritics ASAP2460 physical and chemical adsorption device, Norcross, GA, USA, to ascertain the pore size structure of the catalysts. We subjected the catalyst samples to vacuum and heated them at 150 °C for 4–6 h to remove any gases. Following the degassing process, the sample tube was immersed in a liquid nitrogen environment to analyze the catalysts' pore size distribution.

3.3.3. NH_3-TPD Analysis

We conducted NH3-TPD characterization experiments using the Autochem II 2920 chemical adsorption equipment, Micromeritics, Norcross, GA, USA, to assess the level of acidity on the catalyst surface. We obtained a catalyst sample weighing 0.1 g and subjected it to pre-treatment at a temperature of 120 °C for a duration of 1 h. Then, we utilized a mixture consisting of 10% ammonia and helium for the process of adsorption. We gradually increased the temperature to 600 °C at a rate of 10 °C per minute to remove ammonia, and measured the ammonia desorption curve using TCD.

3.3.4. XPS Analysis

An analysis of the chemical states of Co was conducted using X-ray photoelectron spectroscopy (ESCALAB250, Thermo VG, Waltham, MA, USA) with an Al Kα radiation

source. Each data point was calibrated using adventitious carbon (C1s = 284.8 eV) and analyzed for peak differentiation and simulation using XPS-Peak software 4.1.

3.3.5. FI-IR Analysis

The IRAffinity-1S Fourier Transform Infrared Spectrometer, manufactured by Shimadzu Corporation in Kyoto, Japan, is capable of both quantitative and qualitative analysis of the primary constituents of catalysts. The scanning backdrop consists of potassium bromide. The ratio of catalyst to potassium bromide is 1:200. The tablet is compressed at a pressure of 1.75 MPa for a duration of 1 min. Once pressed, the tablet is inserted into the device for the purpose of scanning the sample.

3.3.6. Py-IR Analysis

We conducted Py-IR characterization experiments on the Tensor 27 infrared spectrometer, Bruker, Billerica, MA, USA, to identify the acidic sites present on the surface of the catalyst. Following pre-treatment, the material was compressed into thin sheets and exhibited adsorption of pyridine at room temperature. The temperature was set to rise at a rate of 1 °C per minute until it reached the desired measurement temperature. The fixed-point temperatures are 100 °C, 200 °C, and 300 °C. This temperature increase was maintained for a duration of 0.5 h during the vacuum desorption process. The specimen was subjected to cooling until it reached the ambient temperature, and subsequently, the spectrum was documented.

3.4. Experimental Setup

Figure 11 shows the fixed-bed reactor. Before starting the experiment, we purged the entire line with N_2. We removed the reaction tube and cleaned it with an aqueous solution of ethanol, blow dried it, and reinstalled the line. The lower end of the reaction tube was filled with quartz sand, 8 g of the catalyst was loaded in the middle of the tube, and the upper end was filled with quartz sand to keep the catalyst in the constant temperature zone of the reaction tube. Once the unit was installed, the line was pressurized with N_2, slightly above the reaction pressure, which was adjusted to the reaction pressure using a backpressure valve at the end of the unit. The mixed C4 feedstock was pressed into the reaction unit with an advection pump and underwent an oligomerization reaction in the presence of the catalyst. The liquid phase product was collected from the bottom of the gas–liquid separation tank and the gas phase product was collected in a gas bag. The composition of the reaction products was determined by using the area normalization method.

3.5. Product Analysis

A gas phase product analysis was conducted using a Foley 9790II gas chromatograph (Zhejiang Fuli Analytical Instrument Co., Ltd., Wenling, China) equipped with an Agilent HP-AL/S (50 m × 0.535 mm × 15 μm) packed column specifically designed for Al_2O_3. The gas phase components that underwent the reaction were gathered using a gas phase collection bag employing a manual injection technique, with a gas phase injection volume of 50 μL. The precise analytical conditions were as follows: the temperature of the column was set at 80 °C, the temperature of the vapor chamber was set at 100 °C, and the temperature of the detector was set at 260 °C.

An examination of the liquid phase product was conducted using an Agilent GC7890 chromatograph (Beijing, China) equipped with an HP-5 column of 50 m in length, 0.2 mm in diameter, and with a particle size of 0.5 μm. We retrieved 2 milliliters of the liquid product resulting from oligomerization and transferred it into an injection vial. We modified the number of injections and sample names using a chromatography autosampler that has an injection volume of 1 microliter. The analytical settings were as follows: The initial temperature of the column chamber was set at 60 °C and scheduled to increase to 240 °C. Both the vapor chamber and detector temperatures were maintained at 280 °C. The area normalization approach was employed to compute the composition of the product.

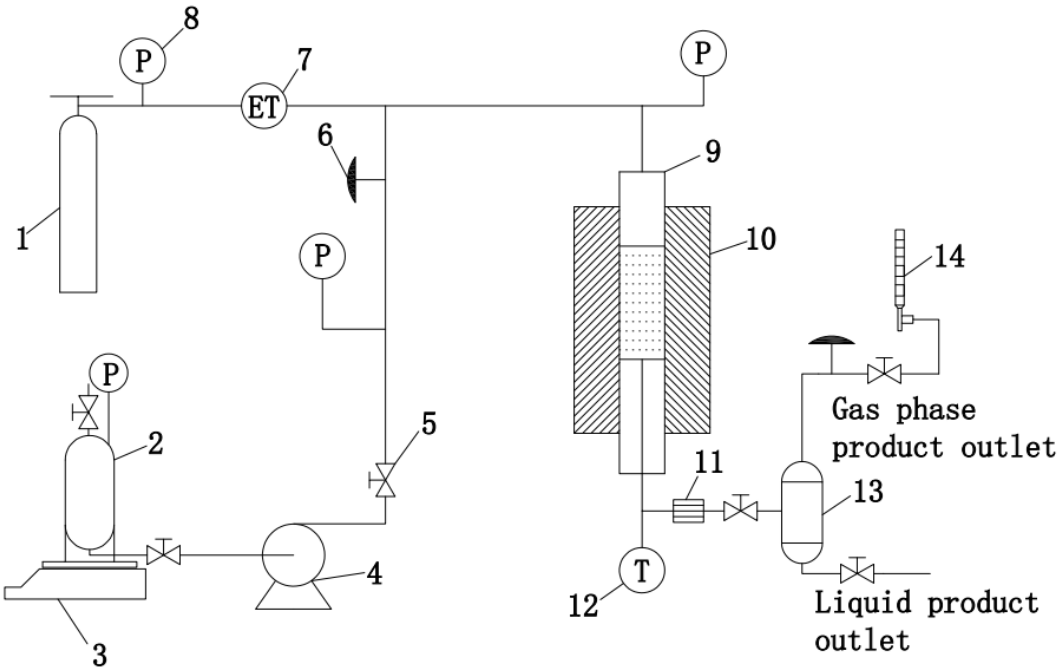

1-N2 cylinder; 2-mixed C4 raw material tank; 3-platform scale; 4-raw material pump; 5-shut-off valve; 6-back pressure valve; 7-mass flowmeter; 8-pressure gauge; 9-reaction tube; 10-heating jacket; 11-filter; 12-thermocouple; 13-gas-liquid separation tank; 14-soap film flowmeter

Figure 11. Fixed-bed reactor.

The isobutylene conversion and n-butene loss rates are calculated using Equations (1) and (2), respectively, assuming that alkanes are not involved in the reaction:

$$X_1 = (Y_1 - Z_1/Z_2 * Y_2)/Y_1 * 100 \quad (1)$$

$$X_2 = (W_1 - Z_1/Z_2 * W_2)/W_1 * 100 \quad (2)$$

where X_1 is the conversion of isobutylene (%); X_2 is the loss of n-butene (%); Y_1 is the mass fraction of isobutylene in the pre-reaction system (%); Y_2 is the mass fraction of isobutylene remaining after the reaction (%); Z_1 is the mass fraction of all alkanes in the pre-reaction system (%); Z_2 is the mass fraction of all alkanes in the post-reaction system (%); W_1 is the sum of the mass fractions of 1-butene, trans-2-butene, and cis-2-butene in the pre-reaction system (%); W_2 is the sum of the mass fractions of 1-butene, trans-2-butene, and cis-2-butene in the post-reaction system (%).

The selectivity of the oligomerization product is calculated by Equation (3):

$$S_j = \frac{N_j}{\sum N_j} \quad (3)$$

S_j is the selectivity of component j in the oligomerization product (%); N_j is the content of component j in the liquid phase product (g).

The yield is calculated using Equation (4):

$$w = XS \quad (4)$$

where w is the yield; X represents the conversion rate; S represents the selectivity.

4. Conclusions

We prepared a series of loaded Co/BETA molecular sieve catalysts impregnated with Co $(NO_3)_2$ on a BETA molecular sieve and used them for the selective oligomerization reaction of isobutylene in mixed C4. The effects of their physicochemical properties and their catalytic performance were investigated. Among all of the prepared catalysts, the catalyst with a BETA molecular sieve as the carrier and 6% Co as the active component showed the optimum n-butene inhibition activity. The lower inhibitory activity was attributed to the Co^{3+} active site on the 6% Co catalyst. These active sites alter the Lewis sites on the catalyst through Co-O bonding as a means to modulate the acidity of the BETA molecular sieve surface. It efficiently prevents the equilibrium between the dissociation of butene and the insertion of butene to facilitate the process of C8 oligomerization. Furthermore, the presence of the 6% Co catalyst significantly contributed to the suppression of C12 formation, mostly due to the presence of its extensively scattered Co_3O_4 species. It efficiently halts the proliferation of conglomerated chains. The findings indicate that the optimal catalytic performance is obtained with a cobalt loading of 6%, a reaction temperature of 60 °C, a reaction pressure of 1 MPa, and a reaction air speed of 1 h^{-1}. The isobutylene conversion achieved a rate of 74%, while the selectivity for $C8^{=}$ was approximately 70%. The yield of $C8^{=}$ reached 51.69% with minimal loss of n-butene, indicating a high level of catalytic ability and efficiency. In this study, a catalytic system for the selective oligomerization of isobutene with simple preparation is proposed, which provides an idea for further exploration of a loaded catalyst with a high isobutene conversion rate and a low n-butene loss rate, and will also provide a reference for the high-value utilization of mixed C4 feedstocks.

Author Contributions: Conceptualization, S.X.; Software, H.T.; Data curation, P.Y.; Writing—original draft, X.C. All authors have read and agreed to the published version of the manuscript.

Funding: This research was funded by the Key Research and Development Plan of Shandong Province (Major Scientific and Technological Innovation Project) (2021ZDSYS24) and the Science Fund of Shandong Laboratory of Advanced Materials and Green Manufacturing at Yantai (Yantai) (AMGM2023A09).

Data Availability Statement: Data are contained within the article.

Conflicts of Interest: The authors declared that they have no conflicts of interest to this work. We declare that we do not have any commercial or associative interest that represents a conflict of interest in connection with the work submitted.

References

1. Liu, S.; Shang, J.; Zhang, S.; Yang, B.; Deng, Y. Highly efficient trimerization of isobutylene over silica-supported chloroaluminate ionic liquid using C4 feed. *Catal. Today* **2013**, *200*, 41–48. [CrossRef]
2. Díaz, M.; Epelde, E.; Valecillos, J.; Izaddoust, S.; Aguayo, A.T.; Bilbao, J. Coke deactivation and regeneration of HZSM-5 zeolite catalysts in the oligomerization of 1-butene. *Appl. Catal. B Environ.* **2021**, *291*, 120016. [CrossRef]
3. Díaz, M.; Epelde, E.; Aguayo, A.T.; Bilbao, J. Low-pressure oligomerization of 1-butene to liquid fuels on HZSM-5 zeolite catalysts: Effect of operating conditions. *J. Ind. Eng. Chem.* **2020**, *87*, 234–241. [CrossRef]
4. Fernandez-Morales, J.M.; Castillejos, E.; Asedegbega-Nieto, E.; Dongil, A.B.; Rodriguez-Ramos, I.; Guerrero-Ruiz, A. Comparative Study of Different Acidic Surface Structures in Solid Catalysts Applied for the Isobutylene Dimerization Reaction. *Nanomaterials* **2020**, *10*, 1235. [CrossRef]
5. Cao, P.; Zheng, L.; Sun, W.; Zhao, L. Multiscale Modeling of Isobutane Alkylation with Mixed C4 Olefins Using Sulfuric Acid as Catalyst. *Ind. Eng. Chem. Res.* **2019**, *58*, 6340–6349. [CrossRef]
6. Malaika, A.; Rechnia-Gorący, P.; Kot, M.; Kozłowski, M. Selective and efficient dimerization of isobutylene over H_3PO_4/activated carbon catalysts. *Catal. Today* **2018**, *301*, 266–273. [CrossRef]
7. Li, J.; Sun, D.; Liu, S.; Tian, H. Preparation of supported Fe_2O_3-Cl/β-zeolite catalyst and its application in the selective oligomerization reaction of isobutylene in mixed C4. *J. Chem. Technol. Biotechnol.* **2022**, *97*, 1893–1899. [CrossRef]
8. Park, D.H.; Kim, S.-S.; Pinnavaia, T.J.; Tzompantzi, F.; Prince, J.; Valente, J.S. Selective Isobutylene Oligomerization by Mesoporous MSU-S_{BEA} Catalysts. *J. Phys. Chem. C* **2011**, *115*, 5809–5816. [CrossRef]
9. Li, J.; Cui, M.; Zhang, Z.; Chen, X.; Liu, Q.; Fei, Z.; Tang, J.; Qiao, X. Promoting di-isobutylene selectivity over ZnO/ZrO_2-SO_4 in isobutylene oligomerization. *Chin. J. Chem. Eng.* **2021**, *38*, 165–171. [CrossRef]

10. Tang, S.; Scurto, A.M.; Subramaniam, B. Improved 1-butene/isobutane alkylation with acidic ionic liquids and tunable acid/ionic liquid mixtures. *J. Catal.* **2009**, *268*, 243–250. [CrossRef]
11. Feller, A.; Zuazo, I.; Guzman, A.; Barth, J.O.; Lercher, J.A. Common mechanistic aspects of liquid and solid acid-catalyzed alkylation of isobutane with n -butene. *J. Catal.* **2003**, *216*, 313–323. [CrossRef]
12. Klerk, A.D.; Leckel, D.O.; Prinsloo, N.M. Butene Oligomerization by Phosphoric Acid Catalysis: Separating the Effects of Temperature and Catalyst Hydration on Product Selectivity. *Ind. Eng. Chem. Res.* **2006**, *45*, 6127–6136. [CrossRef]
13. Antunes, B.M.; Rodrigues, A.E.; Lin, Z.; Portugal, I.; Silva, C.M. Alkenes oligomerization with resin catalysts. *Fuel Process. Technol.* **2015**, *138*, 86–99. [CrossRef]
14. Kriván, E.; Hancsók, J. Oligomerization of Light FCC Naphtha with Ion Exchange Resin Catalyst. *Top. Catal.* **2015**, *58*, 939–947. [CrossRef]
15. Liu, J.; Ding, N.; Ge, Y.; Zhou, X.; Wang, J.A.; Li, C. Dimerization of Isobutylene in C4 Mixtures in the Presence of Ethanol Over Acid Ion-Exchange Resin DH-2. *Catal. Lett.* **2019**, *149*, 1277–1285. [CrossRef]
16. Sun, D.; Liu, S.; Yu, F.; Tian, H.; Zhao, Q. Selective oligomerization of isobutylene in mixed C4 catalyzed by supported $Fe(NO_3)_3/\beta$ catalyst. *J. Chem. Technol. Biotechnol.* **2021**, *96*, 2588–2595. [CrossRef]
17. Yang, J.-B.; Hui, Y.; Qin, Y.-C.; Zhang, X.-T.; Wang, H.; Song, L.-J. Effect of Lewis acid sites of FER zeolite on the catalytic transformation of isobutylene. *J. Fuel Chem. Technol.* **2021**, *49*, 1326–1335. [CrossRef]
18. Yi, F.; Chen, H.; Huang, L.; Hu, C.; Wang, J.; Li, T.; Wang, H.; Tao, Z.; Yang, Y.; Li, Y. Effects of the acidity and shape selectivity of dealuminated zeolite beta on butene transformations. *Fuel* **2021**, *300*, 120694. [CrossRef]
19. Al-Kinany, M.C.; Al-Drees, S.A.; Al-Megren, H.A.; Alshihri, S.M.; Alghilan, E.A.; Al-Shehri, F.A.; Al-Hamdan, A.S.; Alghamdi, A.J.; Al-Dress, S.D. High-quality fuel distillates produced from oligomerization of light olefin over supported phosphoric acid on H-Zeolite-Y. *Appl. Petrochem. Res.* **2019**, *9*, 35–45. [CrossRef]
20. Huo, W.; Liu, W.; Yu, Q.; An, J.; Zhu, X.; Qin, Y.; Li, X. Exploration of Isobutene Oligomerization Reaction on MWW Molecular Sieve. *Chem. Prog.* **2023**, *42*, 5205–5212.
21. Yu, Y.; Zhang, J.; Lv, Z.; Ji, M. The effect of Ni modified HZSM-5 catalyst on isobutene oligomerization in mixed C4. *Ind. Catal.* **2023**, *31*, 63–68.
22. Lv, L.; Wang, H.; Chen, J.; Cao, Y.; Wang, H.; Ren, B.; Zhang, S. Fabrication of Ionic Liquid-Based Pickering Emulsion and Its Enhancement for Tri-isobutylene Formation in Isobutylene Oligomerization. *Ind. Eng. Chem. Res.* **2020**, *59*, 10436–10446. [CrossRef]
23. Chen, J.; Wang, H.; Deng, L.; Wang, H.; Li, Z. Synthesis, characterization, and application of metal-free acidic ionic liquids as catalysts for oligomerization of isobutylene. *Fuel* **2021**, *299*, 120876. [CrossRef]
24. Chen, J.; Li, Z.; Zhu, Y.; Wang, H.; Wang, H. Dual-site eutectic ionic liquids based microemulsion for boosting selective dimerization of isobutylene. *Chem. Eng. Sci.* **2023**, *266*, 118263. [CrossRef]
25. Fütyű, J.; Ispán, D.; Fehér, C.; Szegedi, Á.; Juzsakova, T.; Hancsók, J.; Skoda-Földes, R. Recyclable supported Brønsted acidic ionic liquid catalysts with non-aromatic cations for the oligomerization of isobutylene under mild conditions. *Mol. Catal.* **2022**, *518*, 112075. [CrossRef]
26. Zhang, J.; Ohnishi, R.; Okuhara, T.; Kamiya, Y. Preferential oligomerization of isobutylene in mixtures of isobutylene and 1-butene over 12-tungstosilicic acid supported on silica. *Appl. Catal. A General.* **2009**, *353*, 68–73. [CrossRef]
27. Kocaman, E.; Akarçay, Ö.; Bağlar, N.; Çelebi, S.; Uzun, A. Isobutylene oligomerization on MCM-41-supported tungstophosphoric acid. *Mol. Catal.* **2018**, *457*, 41–50. [CrossRef]
28. Liu, P.; Redekop, E.; Gao, X.; Liu, W.C.; Olsbye, U.; Somorjai, G.A. Oligomerization of Light Olefins Catalyzed by Bronsted-Acidic Metal-Organic Framework-808. *J. Am. Chem. Soc.* **2019**, *141*, 11557–11564. [CrossRef] [PubMed]
29. Fernández-Morales, J.M.; Lozano, L.A.; Castillejos-López, E.; Rodríguez-Ramos, I.; Guerrero-Ruiz, A.; Zamora, J.M. Direct sulfation of a Zr-based metal-organic framework to attain strong acid catalysts. *Microporous Mesoporous Mater.* **2019**, *290*, 109686. [CrossRef]
30. Joanna, D.; Marzena, B.; Patrycja, P.; Adriana, Z.M. Dipicolinate Oxovanadium (IV) Complexes-Well-Defined, Universal Precatalysts for Ethylene Polymerization and Polar Monomers Oligomerization. *Chem. Sel.* **2024**, *9*, e202303255.
31. Yu, P.H.; Luan, C.H.; Cao, M.; Sun, D.H.; Tian, H. Effect of ethanol on selective oligomerization of isobutene and the simulation of reactive distillation process. *Asia Pac. J. Chem. Eng.* **2024**, *18*, e2933. [CrossRef]
32. Yu, Y.; Lv, Z.; Zhong, H.; Bai, W.; Ji, M. Supported Metal Sulfate Catalysts Fe_xZn_y/SiO_2 for Selective Dimerization of Isobutylene in Mixed C4 to Isooctenes. *Eur. J. Inorg. Chem.* **2022**, *26*, e202200631. [CrossRef]
33. Xu, Z.; Chada, J.P.; Zhao, D.; Carrero, C.A.; Kim, Y.T.; Rosenfeld, D.C.; Rogers, J.L.; Rozeveld, S.J.; Hermans, I.; Huber, G.W. Production of Linear Octenes from Oligomerization of 1-Butene over Carbon-Supported Cobalt Catalysts. *ACS Catal.* **2016**, *6*, 3815–3825. [CrossRef]
34. Jonathan, A.; Dastidar, R.G.; Wang, C.; Dumesic, J.A.; Huber, G.W. Effect of catalyst support on cobalt catalysts for ethylene oligomerization into linear olefins. *Catal. Sci. Technol.* **2022**, *12*, 3639–3649. [CrossRef]
35. Jian, J.; Kuang, D.; Wang, X.; Zhou, H.; Gao, H.; Sun, W.; Yuan, Z.; Zeng, J.; You, K.; Luo, H.A. Highly dispersed Co/SBA-15 mesoporous materials as an efficient and stable catalyst for partial oxidation of cyclohexane with molecular oxygen. *Mater. Chem. Phys.* **2020**, *246*, 122814. [CrossRef]

36. Selvaraj, M.; Lee, T.G. Direct Synthesis of Well-Ordered and Unusually Reactive MnSBA-15 Mesoporous Molecular Sieves with High Manganese Content. *J. Phys. Chem. B* **2006**, *110*, 21793–21802. [CrossRef]
37. Wang, C.; Lim, S.; Du, G.; Loebicki, C.Z.; Li, N.; Derrouiche, S.; Haller, G.L. Synthesis, Characterization, and Catalytic Performance of Highly Dispersed Co-SBA-15. *J. Phys. Chem. C* **2009**, *113*, 14863–14871. [CrossRef]
38. Deng, R.; You, K.; Yi, L.; Zhao, F.; Jian, J.; Chen, Z.; Liu, P.; Ai, Q.; Luo, H.A. Solvent-Free, Low-Temperature, Highly Efficient Catalytic Nitration of Toluene with NO_2 Promoted by Molecular Oxygen over Immobilized $AlCl_3$–SiO_2. *Ind. Eng. Chem. Res.* **2018**, *57*, 12993–13000. [CrossRef]
39. Bin, F.; Song, C.; Lv, G.; Song, J.; Cao, X.; Pang, H.; Wang, K. Structural Characterization and Selective Catalytic Reduction of Nitrogen Oxides with Ammonia: A Comparison between Co/ZSM-5 and Co/SBA-15. *J. Phys. Chem. C* **2012**, *116*, 26262–26274. [CrossRef]
40. Alegre, C.; Busacca, C.; Di Blasi, A.; Di Blasi, O.; Aricò, A.S.; Antonucci, V.; Modica, E.; Baglio, V. Electrospun carbon nanofibers loaded with spinel-type cobalt oxide as bifunctional catalysts for enhanced oxygen electrocatalysis. *J. Energy Storage* **2019**, *23*, 269–277. [CrossRef]
41. Huang, Y.; Hu, Z.; Huang, L.-a.; Wang, Z.; Lin, Z.; Shen, S.; Zhong, W.; Pan, J. Phosphorus-modified cobalt single-atom catalysts loaded on crosslinked carbon nanosheets for efficient alkaline hydrogen evolution reaction. *Nanoscale* **2023**, *15*, 3550–3559. [CrossRef] [PubMed]